FEBS Letters 587 (2013) 690–697

journal homepage: www.FEBSLetters.org

# HPV E6 induces eIF4E transcription to promote the proliferation and migration of cervical cancer

Sen Wang [a,1], Tianyun Pang [a,b,1], Min Gao [a,c,1], Haixian Kang [a], Weibin Ding [a], Xiwen Sun [a], Yi Zhao [d], Wei Zhu [a], Xudong Tang [e], Yunhong Yao [f], Xinrong Hu [a,f,g,*]

[a] Cancer Institute of Guangdong Medical College, No. 1 Xincheng Road, Dongguan, Guangdong Province 523808, PR China
[b] Obstetrics and Gynecology Department of the First Affiliated Hospital of Guangdong Medical College, PR China
[c] People's Hospital of Dongguan, Guangdong Province 523059, PR China
[d] Microbiology and Immunology Department of Guangdong Medical College, PR China
[e] Biochemistry Department of Guangdong Medical College, PR China
[f] Pathology Department of Guangdong Medical College, PR China
[g] Molecular Pathology Department of Guangdong Medical College, PR China

ARTICLE INFO

*Article history:*
Received 11 November 2012
Revised 9 January 2013
Accepted 9 January 2013
Available online 11 February 2013

Edited by Veli-Pekka Lehto

*Keywords:*
eIF4E
Cervical cancer
Human papillomavirus
HPV
E6

ABSTRACT

**Increasing evidence has placed eukaryotic translation initiation factor 4E (eIF4E) at the hub of tumor development and progression. Several studies have reported that eIF4E is over-expressed in cervical cancer; however, the mechanism remains elusive. The results of this study further confirm over-expression of eIF4E in cervical cancer tumors and cell lines, and we have discovered that the transcription of eIF4E is induced by protein E6 of the human papillomavirus (HPV). Moreover, regulation of eIF4E by E6 significantly influences cell proliferation, the cell cycle, migration, and apoptosis. Therefore, eIF4E emerges as a key player in tumor development and progression and a potential target for CC treatment and prevention.**


## 1. Introduction

A growing body of evidence indicates that translational regulation plays a critical role in the control of cell proliferation and growth. Eukaryotic translation initiation factor 4E (eIF4E) is a key player in translational control. As a rate-limiting molecule, eIF4E is critical in the process of cap-dependent translation initiation. Thus, it has been considered one of the main switches controlling eukaryotic translation [1]. The human eIF4E gene is located on chromosome 4q21–q25 and encodes a 24-kD polypeptide. EIF4E also appears to be a cap binding protein (CBP); it specifically recognizes the cap structure of mRNA and regulates mRNA translation in many key steps, such as bringing mRNA to the 43S initiation complex and unraveling the secondary structure of 5′ untranslated regions (5′-UTRs). The eIF4E molecule selectively transports specific mRNAs of vascular endothelial growth factor (VEGF), cyclin D1, and ornithine decarboxylase (ODC) from nucleus to cytoplasm for translation.

This recently discovered oncogene, EIF4E, has been found to contribute to tumor occurrence and development. It is over-expressed in squamous cell carcinoma of the head and neck, breast cancer, bile duct cancer, and other tumors [2,3]. eIF4E is also associated with tumor occurrence, invasion, and metastasis [2,3]. Over-expressed eIF4E can unlock the long and highly structured 5′-UTRs of weak mRNA in tumor cells. This ability results in the enhanced expression of weak mRNA from the genes of c-myc, p53, cyclinD1, TGF-β, VEGF, and MMP9 [4]. These targeted molecules then participate in cancer development and metastasis by promoting cell proliferation, transformation, and angiogenesis. Although eIF4E control of the translation of many oncogenes and growth factors has been well studied, the upstream regulation of eIF4E itself remains poorly studied, especially in some specific tumors such as human papilllomavirus (HPV)-related cervical cancer (CC).

Few studies have been conducted on the relationship between eIF4E and CC. Van Tranppen et al. [5] analyzed eIF4E over-expression in CC tissues using RT-PCR and speculated that eIF4E has a large part in the development of CC. Lee et al. [6] further

* Corresponding author. Fax: +86 769 22896401.
*E-mail address:* hxrktz@gmail.com (X. Hu).
[1] These authors contribute equally to this work.

0014-5793/$36.00 
http://dx.doi.org/10.1016/j.febslet.2013.01.042

demonstrated through immunohistochemistry (IHC) that eIF4E expression is significantly enhanced following the progression of cervical malignant lesions. However, little attention has been focused on the mechanism of eIF4E over-expression in CC.

Cervical cancer has the second highest incidence among malignant tumors in females. Because HPV DNA is detected in almost all CC tissues [7,8], it has been generally accepted that HPV infection is an essential factor causing CC and precancerous lesions.

HPV E6 is one of the most important carcinogenic molecules encoded by high-risk HPV DNA. E6 protein is composed of 151 amino acid residues, contains two zinc-finger structures, each including two C-X-X-C sequences, and plays a crucial role in the occurrence and development of CC through direct and/or indirect molecular interactions. For example, E6 suppresses the activity of p53 and the PDZ family of signaling proteins and promotes the activity of telomerase [9]. We hypothesize that eIF4E over-expression in CC is caused by the HPV virus oncogene E6. Until now, no research on this issue has been published. In this study, we aimed to confirm that E6 regulates eIF4E transcription and, in turn, the cell biology of CC. Our results help elucidate the mechanisms of eIF4E over-expression in CC and add to the knowledge base concerning E6 carcinogenesis in CC, which will provide new targets for CC diagnosis and treatment.

## 2. Materials and methods

### 2.1. Clinical specimens

During 2009–2011, a total of 98 specimens were collected from the Pathology Department of the Affiliated Hospital of Guangdong Medical College, Guangdong Province, China. Diagnoses were confirmed by at least two pathologists. Among these specimens, 21 were from cases of chronic cervicitis, 25 were from cases of cervical intraepithelial neoplasia stage I (CIN I), 31 were from cases of CIN stage II or III (CIN II–III), and 21 were from cases of cervical squamous cell carcinoma (SCC).

### 2.2. Cell lines and transfection

Two CC cell lines, HPV-positive Hela and HPV-negative C33A were used in this study. The cells were grown in standard culture medium (RPMI 1640 containing 10% FBS, 2 mmol/L L-glutamine, 50 U penicillin and 50 μg/ml streptomycin) at 37 °C under a 5% $CO_2$ atmosphere.

The liposome method was employed for the gene transfection. In the experiment, cells were divided into three groups: the untreated (mock) group, the negative control (NC) group, and the treated group. A volume of 25 μl Lipofectamine™ 2000 (Invitrogen, Guangzhou, China) reagent was used per migrogram of DNA.

### 2.3. eIF4E immunohistochemistry and immunocytochemistry

Immunohistochemical labeling of 4-μm-thick, formalin-fixed, paraffin-embedded sections of cervical tissue was achieved using mAbs specific for eIF4E (1:25, Santa Cruz, California, USA). IHC was performed as previously described [10]. The sections were pre-treated using the heat-mediated antigen retrieval method with sodium citrate buffer for 20 min. Detection was performed using a horseradish peroxidase (HRP)-conjugated compact polymer system (Zhongshanjinqiao Biological Technology Ltd. Co., Beijing, China). The sections were finally counterstained with haematoxylin. For the negative control, phosphate-buffered saline (PBS) was used instead of the first antibody. Sections labeled with eIF4E antibody were incubated at 4 °C overnight. A DAB chromogenic reagent kit (Zhongshanjinqiao Biological Technology) was used for visualization. A spacer-protein (SP) labeling method [11,12] was used for IHC. In the experiment, a positive control and a PBS negative control were applied to each group.

### 2.4. Plasmids and small interference RNAs

shE6 interference plasmids were constructed by Genechem Compan, Shanghai. Three pairs of shE6 (HPV16) sequences were shE6-1 (stem: CCTACAAGCTACCTGATCT, loop: AGTGAAGCCACAGATGTA, stem: AGATCAGGTAGCTTGTAGG); shE6-2 (stem: GGAACTTACAGAGGTATTT, loop: AGTGAAGCCACAGATGTA, stem: AAATACCTCTGTAAGTTCC); and shE6-3 (stem: GCAGAGAAACACAAGTATA, loop: AGTGAAGCCACAGATGTA, stem: TATACTTGTGTTTCTCTGC). E6 and E6 mutant expression plasmids were constructed using the pEGFP-C5 vector as described previously [13]. E6 contained the wild-type E6 of HPV16. The E6 mutant contained a point mutation (G to T) at nt 138 as well as a deletion mutation of 15 nts from nt 348 to nt 363 of E6.

Small interference RNA of eIF4E (sieIF4E) was synthesized by GenePharma Co., Ltd. (Shanghai, China). The sieIF4E was received as desalted, deprotected oligonucleotides. The sequences of sieIF4E were 5′-GGAUAUUAUAAAUAGAUUATT-3′, reverse 5′-UAAUCUAUUUAUAAUAUCCTT-3′. Normal control (NC) sequences were 5′-UUCUCCGAACGUGUCACGUTT-3′, reverse 5′-ACGUGACACGUUCGGAGAATT-3′.

### 2.5. Detection of E6 and eIF4E mRNA by RT-PCR and real-time PCR

The primer sequences were 5-CGAACCGTTGAATCCAGCAGAA-3′, reverse 5′-CGAACCGTTGAATCCAGCAGAA-3′ for E6; 5′-CTGCGGCTGATCTCCAAG-3′, 5′-CTGCGGCTGATCTCCAAG-3′ for eIF4E; 5′-GAAGGTCGGAGTCAACGGATTT-3′, 5′-CCTGGAAGATGGTGATGGGATT-3′ for GAPDH (as the internal control).

RT-PCR was performed using the Access RT-PCR Kit (Promega Corporation, WI, USA) according to the manufacturer's protocols on the GeneAmp PCR System 9700 (Applied Biosystems, Foster City, CA, USA). For eIF4E amplification, 0.05 μg total RNA was used in 20 μl RT-PCR, and the reaction was carried out at 48 °C for 45 min (RT), 95 °C for 2 min (initial denaturation), 30 cycles of denaturation at 95 °C for 30 s, annealing at 54 °C for 30 s, with an extension at 72 °C for 7 min.

Real-time PCR for amplification and detection of DNA was performed on the 7500 Real-Time PCR ABI system (Applied Biosystems), using a 96-well plate format. PCR was carried out in triplicate in a 25-μL reaction volume containing 12.5 μl Platinum® SYBR®Green qPCR SuperMix-UDG (Invitrogen, Guangzhou, China), 0.5 μl forward primer (10 μM), and 0.5 μl reverse primer (10 μM). The reaction conditions for amplification of DNA were 95 °C for 2 min, followed by 40 cycles of 95 °C for 15 s and 60 °C for 1 min. Data were analyzed using the sequence detection software version 1.6.3 acquired from Applied Biosystems.

### 2.6. CCK-8 cell proliferation assay

Cell proliferation was determined using a Cell Counting Kit-8 (CCK-8) according to the manufacturer's protocol (Beyotime Institute of Biotechnology, Shanghai, China). CCK-8 allows convenient assays using reagent WST-8. WST-8 is bio-reduced by cellular dehydrogenases to an orange formazan product that is soluble in medium. The amount of formazan produced is directly proportional to the number of living cells. The detection sensitivity of CCK-8 is higher than any other tetrazolium salts, such as MTT, XTT, or MTS. Here, Hela or C33A cell suspension was inoculated in a 96-well plate ($10^4$ cells/well). After culture, the plate was pre-incubated in a humidified incubator (at 37 °C, 5% $CO_2$). A volume of 10 μl CCK-8 solution was added to each well of the plate, and the incubation was continued for an additional 2 h. The

experiment was performed in (at least) triplicate wells. The absorbance of the wells was measured using a micro-plate reader. Cell proliferation ability was represented by the mean absorbance value (AV). Using the mean absorbance value, the proliferation rate and inhibition rate were calculated as follows: proliferation rate (%) = $AV_{treated}/AV_{mock} \times 100\%$; inhibition rate (%) = $(1 - AV_{treated}/AV_{mock}) \times 100\%$.

### 2.7. Cell cycle assay and apoptosis assay

Cell cycle and apoptosis were evaluated by flow cytometry. The cultured cells were digested in 0.25% trypsin for 1 min. After termination of the digestion by adding equal culture medium, the samples were centrifuged at 1500 rpm for 5 min, rinsed twice with PBS, and then fixed in 70% ethanol at 4 °C overnight. After fixation, cells were washed twice at room temperature with 1 ml of wash buffer (PBS + 0.1% BSA) following centrifugation at 10000 rpm for 1 min, and the pellets were resuspended in the wash buffer. In 300 μl PBS, approximately $3 \times 10^5$ cells were stained with 3 μl propidium iodide (PI) at 4 °C for 30 min for cell cycle assay and with 3 μl annexin V-FITC at room temperature for 10 min for apoptosis assay. The cells were then analyzed using MultiCycle software (Becton Dickinson, San Jose, CA, USA) using the FACS Canto™ flow cytometer (Becton Dickinson).

### 2.8. Transwell migration assay

Cell migration was determined after gene transfection using a transwell system. Approximately $6.0 \times 10^4$ cells were vaccinated into the upper surface of the transwell membrane and cultured at 37 °C under a 5% $CO_2$ atmosphere for 24 h, 48 h, and 72 h. The number of cells that migrated to the lower surface of the membrane was counted under a microscope (200× magnification).

### 2.9. Statistical analysis

Statistical software SPSS version 17.0 (SPSS, Inc., Chicago, IL, USA) was used to perform the statistical analyses. The chi-squared test, Spearman rank correlation, and one-way analysis of variance (ANOVA) were used.

## 3. Results

### 3.1. Expression of eIF4E in different degrees of cervical tumors

To investigate the relationship between eIF4E and cervical lesions, eIF4E expression in the cervical lesions was tested. Cells positive (+) for eIF4E expression displayed yellow and brown granules in the cytoplasm and nucleus, but cells negative (−) for eIF4E expression showed no staining at all (Fig. 1). The positive expression rates of eIF4E were 9.5% in chronic cervicitis, 40.0% in CIN I, 61.3% in CIN II–III, and 90.5% in SCC, with significant differences between any two groups except CIN I versus CIN II–III (Table 1).

### 3.2. E6 mRNA expression was inhibited effectively by shE6s

The shRNA fragments targeting E6 (shE6s) were synthesized, and shE6 vectors with green fluorescent protein (GFP) were constructed. Sequence analysis showed that the fragments were inserted correctly in the plasmid. Then the recombinant plasmids were transfected into Hela cells. Green fluorescence was observed at 12 h, 24 h, 36 h, and 48 h in Hela cells under a fluorescence microscope. GFP expression rates were 17.2% (24 h) and 41.6% (48 h), as determined by flow cytometric detection. Therefore, the transfection was successful.

Forty-eight hours after the transfection, the E6 mRNA level in the NC group was similar to that in the mock group, as detected

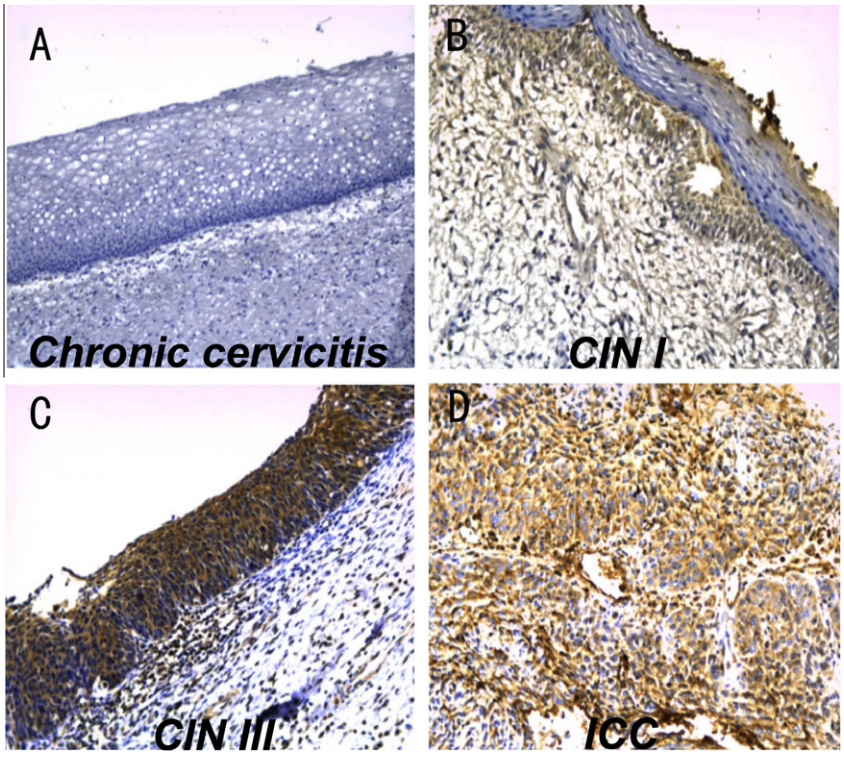


**Fig. 1.** Expression of eIF4E in cervical lesions. Immunohistochemical staining. (A) chronic cervicitis (−); (B) CINI (+); (C) CINIII (+); (D) ICC (+). All images were magnified 200×.

**Table 1**
Expression of eIF4E in cervical lesions.

| Group | Total | eIF4E | | |
|---|---|---|---|---|
| | | Positive | Positive rate (100%) | |
| Cervicitis | 21 | 2 | 9.5 | a |
| CIN I | 25 | 10 | 40 | b |
| CIN II–III | 31 | 19 | 61.3 | c |
| ICC | 21 | 19 | 90.5 | d |

Comparisons between a, b, c and d: $\chi^2 = 30.076$, $P < 0.001$. a versus b: $\chi^2 = 5.498$, $P < 0.05$; a versus c, $\chi^2 = 13.935$, $P < 0.001$. a versus d: $\chi^2 = 27.524$, $P < 0.001$. b versus c: $\chi^2 = 2.512$, $P > 0.05$. b versus d: $\chi^2 = 12.481$, $P < 0.001$. c versus d: $\chi^2 = 5.420$, $P < 0.05$.

by both real-time PCR and RT-PCR. According to real-time PCR detection, shE6-1∼3 significantly inhibited of E6. Among the treated groups, shE6-3 displayed the highest E6 inhibition rate, approximately 81.0% ($P < 0.001$) compared with the NC group (Fig. 2A). In the RT-PCR and agarose gel detection, two distinct bands with expected sizes were observed for the E6 gene (137 bp) and the gene (224 bp) in all groups (Fig. 2B). In the Image J band analysis, E6 mRNA expression level in shE6-2 ($P < 0.05$) and shE6-3 ($P < 0.01$) increased, compared with the NC group, but E6 mRNA expression levels in the shE6-1 groups significantly decreased (Fig. 2B). Among the treated groups, shE6-3 displayed the highest E6 inhibition rate, approximately 80.0%. The results were very similar between the real-time PCR and RT-PCR detections.

### 3.3. E6 knockdown in Hela cells down-regulated eIF4E expression

After shE6 transfection for 48 h, the eIF4E mRNA level in the NC group was similar to that in the mock group, according to the results of both real-time PCR and RT-PCR detection. In real-time PCR detection, eIF4E mRNA levels in shE6-1∼3 groups were significantly decreased compared with those in the NC group ($P < 0.05$). Among the treated groups, shE6-3 showed the highest eIF4E inhibition rate, approximately 76.0% ($P < 0.001$) (Fig. 2C). In the RT-PCR and agarose gel detections, two distinct bands with expected sizes were observed for the eIF4E gene (132 bp) and the GAPDH gene (224 bp) (Fig. 2D). According to Image J band analysis, the eIF4E mRNA level of the shE6-2 group increased compared with the NC group ($P < 0.05$), the eIF4E mRNA level of the shE6-3 group also increased ($P < 0.01$), but the eIF4E mRNA level in the shE6-1 group significantly decreased (Fig. 2D). Among the treated groups, shE6-3 showed the highest eIF4E inhibition rate, approximately 70.0%. The results were similar between the real-time PCR and RT-PCR detections. The change of eIF4E level corresponded to the change of E6 level in the shE6-1∼3 groups.

We used IHC to test eIF4E expression in Hela cells. eIF4E protein was localized in cytoplasm and nucleus, which was stained brown or brownish (Fig. 2E). In the untreated Hela group, the eIF4E posi-

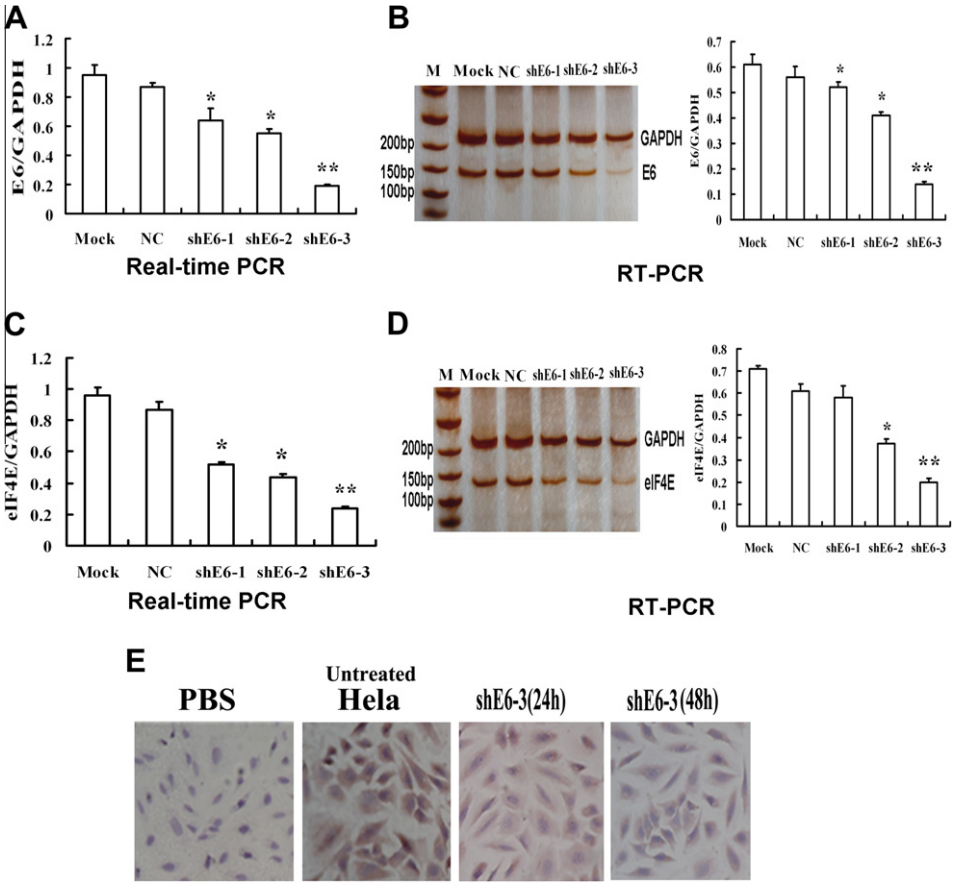


**Fig. 2.** Knockdown of E6 in Hela cells down-regulated eIF4E expression. E6 and eIF4E were normalized with GAPDH. (A) E6 mRNA expression decreased by shE6s at 48 h detected by real-time PCR. (B) Detection of E6 mRNA expression by RT-PCR. (C) eIF4E mRNA expression decreased after E6 knockdown at 48 h detected by real-time PCR. (D) Detection of eIF4E mRNA expression by RT-PCR. (E) eIF4E protein expression decreased in Hela cells at 24 h and 48 h after the transfection of shE6, detected by immunocytochemistry. Mock, untreated Hela cells; NC, blank vector group; PBS, PBS was used to replace eIF4E antibody; Untreated Hela, normal eIF4E level of Hela cells; shE6-3 (24 h), eIF4E staining after 24 h of shE6-3 transfection; shE6-3 (48 h), eIF4E staining after 48 h of shE6-3 transfection. ∗: shE6s versus NC, $P < 0.05$; ∗∗: shE6s versus NC, $P < 0.01$.

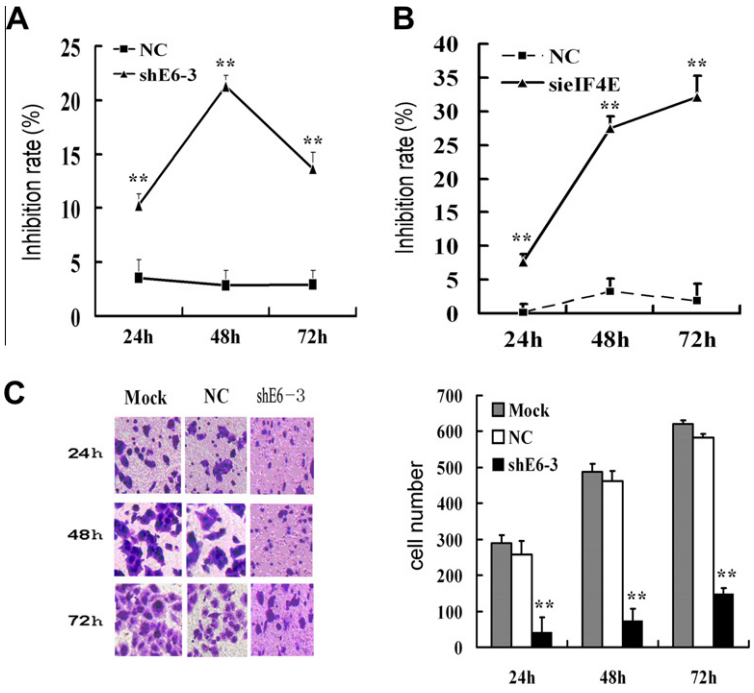


**Fig. 3.** shE6-3 or sieIF4E trasfection negatively influenced Hela cell biology. (A) shE6-3 inhibited the proliferation of Hela cells detected by CCK-8 assay. (B) sieIF4E inhibited the proliferation of Hela cells detected by CCK-8 assay. (C) shE6-3 inhibited the migration of Hela cells detected by transwell assay. Mock, untreated Hela cells; NC, blank vector group; shE6-3, shE6-3 group. **: shE6-3 versus NC, $P < 0.01$.

tive rate of the cells was as much as 96.8%. After shE6-3 transfection for 24 h and 48 h, the eIF4E positive rate of the cells was decreased to 90.49% and 44.05%, respectively. The staining intensity became much weaker in the shE6-3 group than that in the untreated Hela group (Fig. 2E).

### 3.4. shE6 highly inhibited the proliferation and migration of Hela cells and promoted cell apoptosis

Using a CCK-8 assay, the proliferation of Hela cells was detected at 24 h, 48 h, and 72 h after shE6-3 transfection. The cell proliferation between the mock and NC groups was similar. Compared with the NC group, cell proliferation was significantly inhibited in the shE6-3 group ($P < 0.01$) (Fig. 3A). The inhibition rates in the shE6 group were 10.2% (24 h), 21.6% (48 h), and 13.7% (72 h).

Cell cycle distribution was analyzed by flow cytometry. The cell cycle between the mock and NC groups was similar. Compared with the NC group, the cell cycle in the shE6-3 group obviously changed. The G0/G1 phase cell numbers significantly increased by 8.7% (24 h), 17.7% (48 h), and 28.6% (72 h). S phase cell numbers significantly decreased by 7.4% (24 h), 14.6% (48 h) and 28.1% (72 h); G2/M phase cell numbers showed no significant change (Table 2). These outcomes indicate that shE6-3 inhibited the proliferation of Hela cells by arresting cells at G0/G1 phase.

The annexin V-FITC/PI double-staining method was adopted for detecting cell apoptosis. The amount of apoptosis between the mock and NC groups was similar. Compared with the NC group, the ratio of V-FITC$^+$/PI$^-$ cells (early apoptosis cells) in the shE6-3 group was significantly increased by 25.0% (24 h) and 29.7% (48 h), while the ratio of V-FITC$^+$/PI$^+$ cells (late apoptosis cells) increased, but not significantly (Table 3).

sieIF4E inhibited the proliferation of E6-positive Hela cells. Using a CCK-8 assay, cell proliferation was detected at 24 h, 48 h, and 72 h. Cell proliferation between the mock and NC groups was similar. Compared with the NC group, cell proliferation in the sieIF4E group was obviously inhibited ($P < 0.01$) (Fig. 3B). The inhibition rates were 7.6% (24 h), 27.5% (48 h), and 32.1% (72 h). The inhibition rate in the sieIF4E group was close to that in the shE6-3 group at 24 h and 48 h, and at 72 h this rate became higher than that in the shE6-3 group.

To analyze the migration of Hela cells after shE6 transfection, a transwell migration assay was performed. The migrating cell numbers were similar between the mock and NC groups. Compared with the NC group, the migrating cells in the shE6-3 group decreased to 40.92 ± 8.785 (24 h), 72.79 ± 10.337 (48 h), and 148.44 ± 16.696 (72 h) ($P < 0.01$) (Fig. 3C).

**Table 2**
Cell cycle change of Hela cells after shE6 transfection.

| Group | Percentage ($\bar{x} \pm s$, $n = 3$) | | |
|---|---|---|---|
| | G1% | S% | G2% |
| Hela | 33.536 ± 1.108 | 51.329 ± 1.656 | 15.165 ± 1.453 |
| NC | 37.186 ± 1.157 | 48.881 ± 1.604 | 13.967 ± 1.554 |
| shE6-3 (24 h) | 42.263 ± 1.754 | 43.974 ± 1.358 | 13.789 ± 1.603 |
| shE6-3 (48 h) | 51.252 ± 1.352* | 36.647 ± 1.455* | 12.095 ± 1.804 |
| shE6-3 (72 h) | 62.162 ± 1.853* | 23.241 ± 1.652* | 14.621 ± 1.506 |

* shE6 (48 h) versus NC, shE6 (72 h) versus NC, $P < 0.01$.

**Table 3**
Apoptosis change of Hela cells after shE6 transfection.

| Group | Percentage ($\bar{x} \pm s$, $n = 3$) | |
|---|---|---|
| | V-FITC +/PI− | V-FITC +/PI+ |
| Hela | 0.780 ± 0.255 | 0.180 ± 0.168 |
| NC | 11.056 ± 1.256 | 5.818 ± 1.819 |
| shE6-3 (24 h) | 36.001 ± 2.201* | 10.902 ± 1.403 |
| shE6-3 (48 h) | 40.901 ± 3.201* | 10.702 ± 2.503 |

* shE6 (24 h) versus NC, shE6 (48 h) versus NC, $P < 0.01$.

### 3.5. E6 induced eIF4E expression and promoted the proliferation and migration of HPV-negative C33A cells

E6 and mutant E6 expression vectors and the NC vectors were respectively transfected into HPV-negative C33A cells. The mRNAs of E6, mutant E6, and GAPDH were detected by RT-PCR. Three bands with expected sizes for E6 gene (271 bp), mutant E6 gene (256 bp) and GAPDH gene (224 bp) were observed. The E6 band and mutant E6 band were observed in the E6 and mutant E6 groups (E6m) (Fig. 4A, left), respectively. According to the Image J analysis, the mRNA level in the E6 group was similar to the mRNA level in the E6m group. No expression of either E6 or mutant E6 was detected in the mock and NC groups (Fig. 4A, right).

RT-PCR was performed to detect eIF4E mRNA after the transfection of E6 or mutant E6 expression vectors for 20 h. Two bands with expected sizes for the eIF4E gene (132 bp) and the GAPDH gene (224 bp) were seen in all groups. The eIF4E bands were much stronger in the E6 and the E6m groups than in the mock group or the NC group (Fig. 4B, left). According to Image J analysis, the eIF4E mRNA level was similar between the mock and NC groups. Compared with the NC group, eIF4E mRNA increased by 54.3% in the E6m group and by 58.1% in the E6 group ($P < 0.01$) (Fig. 4B, right).

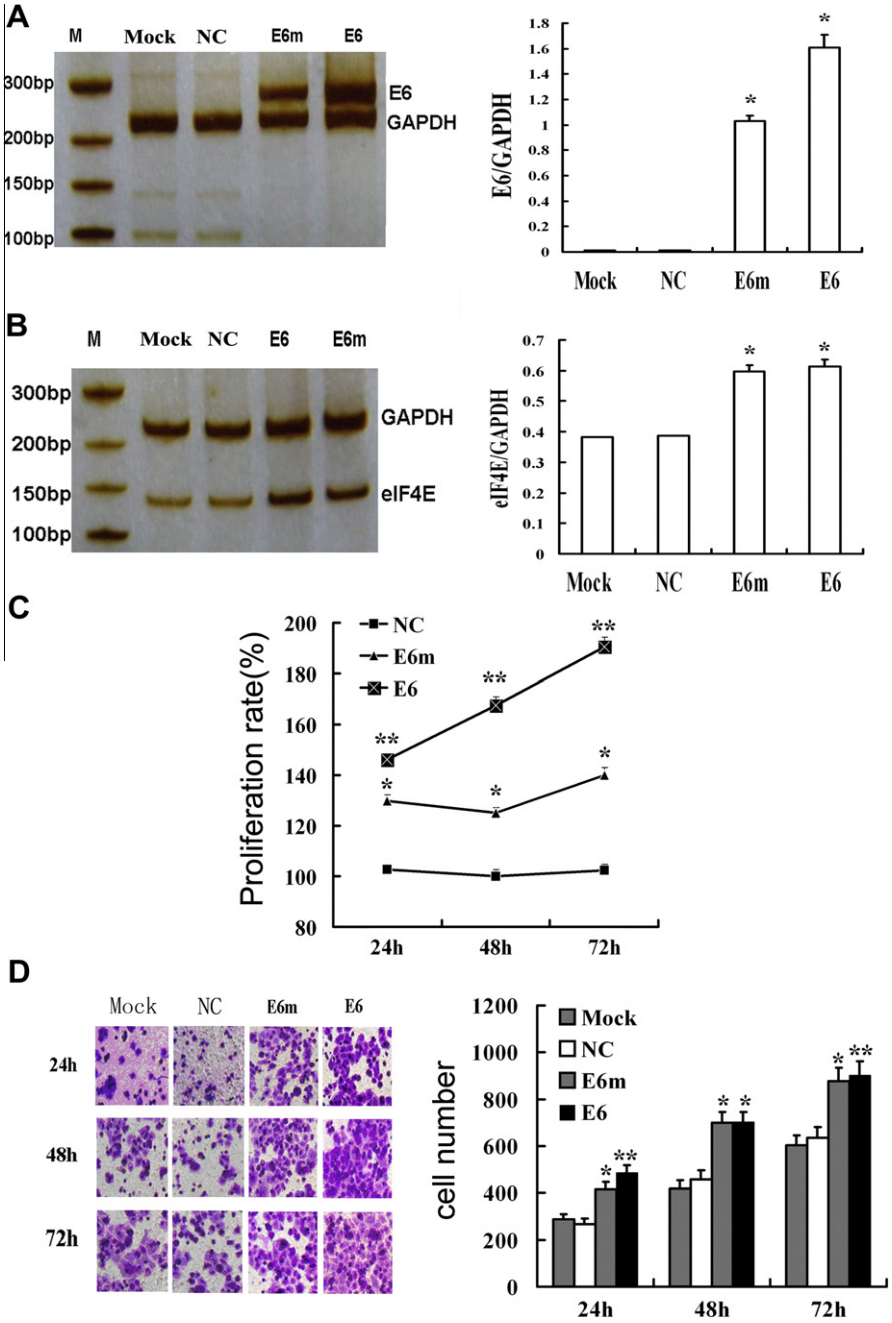


**Fig. 4.** E6 induced eIF4E expression and promoted the proliferation and migration of C33A cells. Cells were divided into four groups: Mock, untreated C33A cell group; NC, pEGFP blank plasmid group; E6m, E6 mutant group; E6, E6 expression vector group. E6 and eIF4E were normalized with GAPDH in RT-PCR. (A) E6 expression at 20 h after E6 expression vector was transfected into C33A cells, detected by RT-PCR. (B) eIF4E expression at 20 h after E6 expression vector was transfected into C33A cells, detected by RT-PCR. (C) Transfection of the E6 gene promoted the proliferation of C33A cells, detected by CCK-8 assay. (D) Transfection of the E6 gene promoted the migration of C33A cells, as detected by a transwell migration assay. *: E6/E6m versus NC, $P < 0.05$; **: E6/E6m versus NC, $P < 0.01$.

These results suggest that E6 induced the expression of eIF4E and that the mutant E6 functioned similarly.

The proliferation of C33A cells after gene transfection is shown in Fig. 4C. By comparison with the NC group, the proliferation rates increased by 29.96% (24 h), 25.07% (48 h), and 39.87% (72 h) in the E6m group ($P < 0.05$) and by 46.10% (24 h), 67.31% (48 h), and 90.51% (72 h) in the E6 group ($P < 0.01$). According to cell migration detection, the numbers of migrating cells in the mock and NC groups were similar at each time point. Compared with the NC group, the migrating cells in the E6 group increased to 487.93 ± 29.687 (24 h), 703.63 ± 42.786 (48 h), and 901.77 ± 60.21 (72 h). The migrating cells in the E6 m group increased to 416.66 ± 31.074 (24 h), 699.71 ± 45.869 (48 h), and 877.03 ± 57.926 (72 h) ($P < 0.01$) (Fig. 4D).

## 4. Discussion

The results of this study show that the over-expression of eIF4E is associated with the malignancy of cervical lesions. Physiologically, a small amount of eIF4E is expressed and contributes to the maintenance of normal cell functions such as the growth, differentiation and apoptosis. Recently, researchers have recognized that the over-expression of eIF4E is usually associated with cancer [2,3]. Studies have shown that the over-expression of eIF4E increases abnormal translation of a series of malignant transformation–related proteins. The molecules then promote cell survival, proliferation, resistance to apoptosis, out of control of malignant transformation, invasion, metastasis, and angiogenesis [14]. In this study, we detected eIF4E expression levels of chronic cervicitis, CIN I, CIN II–III, and cervical squamous cell carcinoma. We found that the positive expression rates of eIF4E increased following the malignant progression of cervical lesions. These results are consistent with the eIF4E RNA levels of Van Tranppen [5] and the eIF4E protein levels of Lee [6]. Our study has further confirmed that the over-expression of eIF4E is closely related to the occurrence and development of CC. These results indicate the potential of eIF4E as an important molecular marker for the diagnosis and therapy of CC.

We conclude that E6 induces eIF4E expression in CC based on the following evidence: (1) down-regulation of E6 decreased eIF4E mRNA and protein levels in HPV-positive Hela cells; (2) the degree of eIF4E down-regulation was correlated with the degree of E6 silence in the transfection experiments with shE6-1, shE6-2, and shE6-3 in Hela cells; and (3) gene transfection with E6 expression plasmids induced eIF4E transcriptional expression in C33A cells (HPV−, eIF4E+). To the best of our knowledge, we are the first to determine conclusively that E6 induces the transcription of eIF4E. This could be one of the mechanisms of the over-expression of eIF4E in CC.

However, whether E6 induces eIF4E transcription directly or indirectly remains unknown. The evidence indicates that E6 might activate eIF4E transcription partly through the P53 gene, the first E6-targeted protein to be discovered. Binding and degradation of p53 are the specific functions of the E6 protein. E6 can recruit E6AP ubiquitin enzymes and bind them to the p53 core area, resulting in the degradation of P53 in HPV-positive cells [15,16]. Secondly, P53 inhibits the transcription of eIF4E by indirectly inhibiting the promoter activity of eIF4E [17]. Studies have found that p53 inhibits eIF4E gene transcription and protein translation. P53 is able to bind c-Myc and remove it from eIF4E promoter region where c-Myc binds and enhances eIF4E transcription [18]. Thus, it is reasonable to infer that E6 induces eIF4E transcription through the P53 pathway. From another perspective, although most of the activities of E6 have been found to be mediated by protein–protein interactions, studies have reported that the HPV E6 proteins could bind specifically to four-way DNA junctions [19]. We cannot ignore the probability that E6 directly up-regulates eIF4E by binding DNA. Our future studies will aim to confirm this hypothesis.

Interestingly, although to a lesser degree, in this study the mutant E6 induced the transcription of eIF4E and increased the proliferation of the cells, as did E6. Compared with the E6 gene, the mutant E6 exhibited a decreased ability to target p53 for degradation [20,21]. Therefore, the residual p53 after E6m-induced degradation might partly affect eIF4E expression and cell proliferation.

Indeed, E6 initiated and promoted the carcinogenesis of CC, probably through eIF4E. We found that E6 transfection into HPV-negative C33A cells increased eIF4E expression, accelerated cell proliferation, and reduced apoptosis. Knocking down E6 or eIF4E in HPV-positive Hela cells caused similar degrees of reduction of cell proliferation and apoptosis resistance. Inhibition of eIF4E expression in Hela cells with high E6 expression caused inhibition of proliferation and cell cycle arrest. These results, taken together, indicate that eIF4E is one of the key players in HPV carcinogenesis.

Furthermore, it is well known that HPV E6 and E7 share a promoter and produce a bicistronic transcript. Therefore, knockdown of E6 or E7 might affect each gene. In this study, we first knocked down E6 in HPV-positive Hela cells and observed the down-regulation of eIF4E and corresponding changes of cell biology. Considering the interactions between E6 and E7, these results may have been caused by a single E6 or by E6/E7. Subsequently, the HPV-negative C33A cells without both E6 and E7 genes were chosen to investigate the effect of a single E6 gene on eIF4E. We transfected C33A cells with an E6 expression vector. As a result, the expression of E6 significantly up-regulated eIF4E in the absence of E7, indicating that E6 induced eIF4E. In addition, the degree of E6-induced eIF4E transcription was similar to the degree of inhibition of eIF4E in the E6 knockdown experiment. This phenomenon indicates that the down-regulation of eIF4E in the first experiment was caused mainly by the knockdown of E6 but not of E7. Thus, we conclude that E6 does induce eIF4E in CC cells.

In conclusion, this study has confirmed eIF4E over-expression in cervical tumors, and we have further determined that the mechanism of eIF4E over-expression is subject to E6 induction. Over-expressed eIF4E influences CC occurrence and development in many aspects, including cell proliferation, cell cycle progression, migration, and apoptosis. Therefore, eIF4E emerges as a key player in the carcinogenesis of HPV-induced cancer and is a potential target for CC therapy.

## Conflict of interest statement

We declare that we have no conflict of interest.

## Acknowledgements

This study was supported by the Project of Department of Education of Guangdong Province (Grant No. 2012KJCX0057), by the National Natural Science Foundation of China (Grant No. 30670860), by the Science & Technology Innovation Fund of Guangdong Medical College (Grant No. STIF201113), by the Guangdong Natural Science Foundation (Grant No. S2012040006383), and by the PhD Start-up Fund of Guangdong Medical College (Grant No. B2011012).

## References

[1] Sonenberg, N. (2008) eIF4E, the mRNA cap-binding protein: from basic discovery to translational research. Biochem. Cell Biol. 86, 178–183.
[2] Graff, J.R., Konicek, B.W., Carter, J.H. and Marcusson, E.G. (2008) Targeting the eukaryotic translation initiation factor 4E for cancer therapy. Cancer Res. 68, 631–634.

[3] Hsieh, A.C. and Ruggero, D. (2010) Targeting eukaryotic translation initiation factor 4E (eIF4E) in cancer. Clin. Cancer Res. 16, 4914–4920.
[4] Zimmer, S.G., DeBenedetti, A. and Graff, J.R. (2000) Translational control of malignancy: the mRNA cap-binding protein, eIF4E, as a central regulator of tumor formation, growth, invasion and metastasis. Anticancer Res. 20, 1343–1351.
[5] Van Trappen, P.O., Ryan, A., Carroll, M., Lecoeur, C., Goff, L., Gyselman, V.G., Young, B.D., Lowe, D.G., Pepper, M.S., Shepherd, J.H. and Jacobs, I.J. (2002) A model for co-expression pattern analysis of genes implicated in angiogenesis and tumour cell invasion in cervical cancer. Br. J. Cancer 87, 537–544.
[6] Lee, J.W., Choi, J.J., Lee, K.M., Choi, C.H., Kim, T.J., Lee, J.H., Kim, B.G., Ahn, G., Song, S.Y. and Bae, D.S. (2005) eIF4E expression is associated with histopathologic grades in cervical neoplasia. Hum. Pathol. 36, 1197–1203.
[7] Ganguly, N. and Parihar, S.P. (2009) Human papillomavirus E6 and E7 oncoproteins as risk factors for tumorigenesis. J. Biosci. 34, 113–123.
[8] McLaughlin-Drubin, M.E. and Munger, K. (2009) Oncogenic activities of human papillomaviruses. Virus Res. 143, 195–208.
[9] McCloskey, R., Menges, C., Friedman, A., Patel, D. and McCance, D.J. (2010) Human papillomavirus type 16 E6/E7 upregulation of nucleophosmin is important for proliferation and inhibition of differentiation. J. Virol. 84, 5131–5139.
[10] Franklin, S., Pho, T., Abreo, F.W., Nassar, R., De Benedetti, A., Stucker, F.J. and Nathan, C.A. (1999) Detection of the proto-oncogene eIF4E in larynx and hypopharynx cancers. Arch. Otolaryngol. Head Neck Surg. 125, 177–182.
[11] Nathan, C.A., Sander, K., Abreo, F.W., Nassar, R. and Glass, J. (2000) Correlation of p53 and the proto-oncogene eIF4E in larynx cancers: prognostic implications. Cancer Res. 60, 3599–3604.
[12] Pavelic, Z., Pavelic, K., Carter, C. and Pavelic, L. (1992) Heterogeneity of c-myc expression in histologically similar infiltrating ductal carcinoma of the breast. J. Cancer Res. Clin. Oncol. 118, 16–22.
[13] Li, G., He, L., Zhang, E., Shi, J., Zhang, Q., Le, A.D., Zhou, K. and Tang, X. (2011) Overexpression of human papillomavirus (HPV) type 16 oncoproteins promotes angiogenesis via enhancing HIF-1α and VEGF expression in non-small cell lung cancer cells. Cancer Lett. 311, 160–170.
[14] Mamane, Y., Petroulakis, E., Rong, L., Yoshida, K., Ler, L.W. and Sonenberg, N. (2004) eIF4E: from translation to transformation. Oncogene 23, 3172–3179.
[15] Nomine, Y., Masson, M., Charbonnierm, S., Zanier, K., Ristriani, T., Deryckere, F., Sibler, A.P., Desplancq, D., Atkinson, R.A., Weiss, E., Orfanoudakis, G., Kieffer, B. and Trave, G. (2006) Structural and functional analysis of E6 onco protein: insights in the molecular pathogenesis. Mol. Cell 21, 665–678.
[16] Massimi, P., Shai, A., Lambert, P. and Banks, L. (2008) HPV E6 degradation of p53and PDZ containing substrates in an E6AP null background. Oncogene 27, 1800–1804.
[17] Zhu, N., Gu, L., Findley, H.W. and Zhou, M. (2005) Transcriptional repression of the eukaryotic initiation factor 4E gene by wild type p53. Biochem. Biophys. Res. Commun. 335, 1272–1279.
[18] Constantinou, C., Elia, A. and Clemens, M.J. (2008) Activation of p53 stimulates proteasome-dependent truncation of eIF4E-binding protein 1 (4E-BP1). Biol. Cell 100, 279–289.
[19] Ristriani, T., Nomine, Y., Masson, M., Weiss, E. and Trave, G. (2001) Specific recognition of four-way DNA junctions by the C-terminal zinc-binding domain of HPV oncoprotein E6. J. Mol. Biol. 305, 729–739.
[20] Duffy, C.L., Phillips, S.L. and Klingelhutz, A.J. (2003) Microarray analysis identifies differentiation-associated genes regulated by human papillomavirus type 16 E6. Virology 314, 196–205.
[21] Foster, S.A., Demers, G.W., Etscheid, B.G. and Galloway, D.A. (1994) The ability of human papillomavirus E6 proteins to target p53 for degradation in vivo correlates with their ability to abrogate actinomycin D-induced growth arrest. J. Virol. 68, 5698–5705.